

AD-A171 435

VALIDATION OF BOUNDING SURFACE PLASTICITY THEORY USING
PRELIMINARY GEOTEC. (U) NAVAL CIVIL ENGINEERING LAB
PORT HUENEME CA C K SHEN ET AL. JUL 86 NCEL-CH-86-011
UNCLASSIFIED N62583-85-M-1176 F/G 8/13

1/1

NL

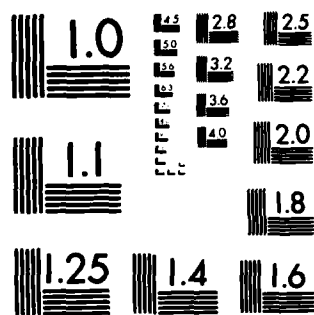
END

DATE

FORMED

10-86

DTN



MICROCOPY RESOLUTION TEST CHART
NATIONAL BUREAU OF STANDARDS-1963-A



CR 86.011

July 1986

NCEL

Contract Report

An Investigation Conducted By
University of California at Davis

Sponsored By Naval Facilities
Engineering Command

AD-A171 435

VALIDATION OF BOUNDING SURFACE PLASTICITY THEORY USING PRELIMINARY GEOTECHNICAL CENTRIFUGE EXPERIMENTS

ABSTRACT A 2-D, plane strain, clay-backfilled, retaining wall model study was performed in the centrifuge. Results compared well with SAC-2 finite element predictions of the model behavior using the bounding surface plasticity formulation. This study provides much needed data base for the validation of the bounding surface plasticity theory to model soft soil behavior and its interaction with structures.

ENC FILE COPY

DTIC
ELECTE
AUG 29 1986
B

NAVAL CIVIL ENGINEERING LABORATORY, PORT HENRIE, CALIFORNIA 93043

86 8 28 075

Unclassified

SECURITY CLASSIFICATION OF THIS PAGE (When Data Entered)

REPORT DOCUMENTATION PAGE		READ INSTRUCTIONS BEFORE COMPLETING FORM
1. REPORT NUMBER CR 86.011	2. GOVT ACCESSION NO. AD-A171435	3. RECIPIENT'S CATALOG NUMBER
4. TITLE (and Subtitle) Validation of Bounding Surface Plasticity Theory Using Preliminary Geotechnical Centrifuge Experiments		5. TYPE OF REPORT & PERIOD COVERED Interim Mar 1985 - May 1986
7. AUTHOR(s) CK Shen, ZY Zhu, LR Herrmann, VN Kaliakin		6. PERFORMING ORG. REPORT NUMBER
9. PERFORMING ORGANIZATION NAME AND ADDRESS Department of Civil Engineering University of California, Davis		8. CONTRACT OR GRANT NUMBER(s) N62583-85-M-T176
11. CONTROLLING OFFICE NAME AND ADDRESS Naval Civil Engineering Laboratory Port Hueneme, CA 93043-5003		10. PROGRAM ELEMENT PROJECT TASK AREA & WORK UNIT NUMBERS 61153N YR023.03.01.008
14. MONITORING AGENCY NAME & ADDRESS (if different from Controlling Office) Naval Facilities Engineering Command 200 Stovall Street Alexandria, VA 22332-2300		12. REPORT DATE July 1986
		13. NUMBER OF PAGES 32
		15. SECURITY CLASS (of this report) Unclassified
		15a. DECLASSIFICATION DOWNGRADING SCHEDULE
16. DISTRIBUTION STATEMENT (of this Report) Approved for public release; distribution is unlimited.		
17. DISTRIBUTION STATEMENT (of the abstract entered in Block 20, if different from Report)		
18. SUPPLEMENTARY NOTES		
19. KEY WORDS (Continue on reverse side if necessary and identify by block number) constitutive model, soil plasticity, bounding surface, geotechnical centrifuge, experiment, finite element		
20. ABSTRACT (Continue on reverse side if necessary and identify by block number) A 2-D, plane strain, clay-backfilled, retaining wall model study was performed in the centrifuge. Results compared well with SAC-2 finite element predictions of the model behavior using the bounding surface plasticity formulation. This study provides much needed data base for the validation of the bounding surface plasticity theory to model soft soil behavior and its interaction with structures.		

DD FORM 1 JAN 73 1473 EDITION OF 1 NOV 65 IS OBSOLETE

Unclassified

SECURITY CLASSIFICATION OF THIS PAGE (When Data Entered)

CONTENTS

	Page
INTRODUCTION	1
CENTRIFUGE MODEL STUDY.....	3
CENTRIFUGE MODEL PACKAGE.....	4
MODEL VALIDATION.....	10
COMPARISON OF EXPERIMENTAL AND ANALYTICAL RESULTS.....	13
CONCLUSION.....	15
REFERENCES.....	17

LIST OF TABLES

Table 1 - SOIL PROPERTIES.....	18
Table 2 - TESTING SEQUENCE.....	19
Table 3 - PARAMETERS DESCRIBING BOUNDING SURFACE MODEL.....	20
Table 4 - TIME STEPS IN FINITE ELEMENT ANALYSIS	21

LIST OF FIGURES

Figure 1 - DIMENSIONS OF SAMPLE BOX.....	22
Figure 2 - INSTRUMENTATION OF THE MODEL PACKAGE.....	22
Figure 3 - MODEL PACKAGE IN THE CENTRIFUGE.....	23
Figure 4 - INSTRUMENTATION AND DATA ACQUISITION BLOCK DIAGRAM.....	24
Figure 5 - EFFECTIVE STRESS DISTRIBUTIONS.....	25
Figure 6 - PORE PRESSURE RESPONSE.....	25
Figure 7 - INTERFACE PRESSURE RESPONSE.....	26
Figure 8 - UNDRAINED COMPRESSION TEST RESULTS.....	27
Figure 9 - UNDRAINED EXTENSION TEST RESULTS.....	28
Figure 10 - ISOTROPIC CONSOLIDATION RESULTS.....	29
Figure 11 - UNDRAINED STRESS PATHS UNDER TRIAXIAL CONDITIONS.....	29
Figure 12 - FINITE ELEMENT GRID.....	30
Figure 13 - IDEALIZED MODEL OF BOND BETWEEN CONTACTING SURFACES.....	30
Figure 14 - MOVEMENT OF RETAINING WALL.....	31

VALIDATION OF BOUNDING SURFACE PLASTICITY THEORY USING PRELIMINARY GEOTECHNICAL CENTRIFUGE EXPERIMENTS

INTRODUCTION

Traditionally, the evaluation and validation of constitutive soil models are limited to comparisons of predicted and experimental results for simple, homogeneous laboratory tests. Such verification processes are often incomplete since the laboratory tests results do not encompass a broad data base including multi-dimensional stress paths and the rotation of principal stress directions. The shortcomings however, may be overcome if centrifuge model test results are used in the verification process. Centrifuge model testing of geotechnical structures can simulate more closely the prototype loading conditions thus introducing complex stress states and paths in the soil model. The first such attempt was made at Davis (1) which involved a centrifuge model study of consolidation and surface settlement of a storage tank placed on a soft clay foundation and subjected to a filling-storage-emptying cycle. The model test results were compared favorably with the finite element predictions to show the predictive capability of the bounding surface plasticity model for clay. During the course of the model test, both loading and unloading of the soil occurred; the stress state in the foundation soil was certainly nonhomogeneous and at most points in the model the principal stress directions changed during the course of the test. The storage tank study was a truly meaningful test of the predictive capability of the theory because validation was carried out for two independent conditions. The finite element prediction of the tank foundation behavior was based upon the bounding surface plasticity model and used parameters of the soil determined from the laboratory undrained triaxial compression and extension test results; the centrifuge model test of the system used the same clay soil. The good agreement of the

comparison from the two separate processes renders credence to the plasticity soil model and the numerical analysis technique for predicting saturated clay behavior.

On the other hand, the circular tank and the uniform loading conditions existing in the centrifuge model are similar to the axisymmetrical stress states in laboratory triaxial specimens. Since laboratory triaxial test results are commonly used for constitutive soil model calibration, one may therefore question if the favorable comparisons of the previous study are due mainly to the close similarity of loading and geometric conditions in both instances. The answer to this lies in the availability of a broader centrifuge model test data base covering different types of structures to reflect different classes of soil-structure interaction (loading) problems. As a continuing effort in building the data base, this report describes a recent centrifuge study of a 2-D plane strain model and the finite element prediction of the model behavior using the bounding surface plasticity formulation.

CENTRIFUGE MODEL STUDY

Small scale laboratory models are severely limited in their applicability to the prediction of full scale geotechnical structural behavior, because when gravity is the principal loading agent, the state of stress in a small scale model loaded by its own weight is much smaller in magnitude than in the corresponding full scale prototype. The difference in stress states causes model behavior that is quite different from that of the prototype since soil response is stress dependent. However, if the model is placed in a centrifuge, and subjected to centripetal acceleration the state of stress at every point in the model can be made the same as the homologous point in the prototype, thus eliminating a major deficiency in model testing of geotechnical structures.

Another important consideration concerning a model study is whether the centrifuge can be used to correctly model field conditions to conform with the scaling laws. This question has been addressed by many researchers (2), and the validity of the results can be checked by modeling of models (3). For the present purpose of constitutive model verification, the finite element analysis is however carried out for the model, not for the field prototype. In other words, the comparison is made strictly on the model structure; the scaling law is therefore not of concern.

DTIC
ELECTE
S **D**
AUG 29 1986
B

Accession	
NTIS	
DTIC	
Unann	
Just	
By	
Dist	
Avail	
Dist	
A-1	



CENTRIFUGE MODEL PACKAGE

In describing the model package, it is necessary at the onset to illustrate the overall testing program. Briefly, the model study is designed to generate response data for a saturated clay backfill under plane strain loading and unloading conditions created by the push and pull of a rigid retaining wall against the backfill soil. The interface contact pressure (pressure on the back face of the rigid wall) and the pore water pressure in the backfill soil due to wall movement are measured. The response of the backfill soil to the wall movement can be separated into two major steps: the undrained loading of the backfill soil and the instant buildup of pore water pressure; the subsequent dissipation of excess pore water pressure and the transfer to intergranular soil pressure with time. Accordingly, the building of the model package requires provisions, 1) for preparing a saturated clay backfill sample behind the rigid wall; 2) for monitoring the magnitude and distribution of pore water pressure and interface contact pressure; and 3) for acquiring data while a model test is in progress under the elevated g-environment.

- A) The Model Box: The 2-D plane strain model was simulated by a retaining wall - backfill system placed in a rectangular model box. The rigid wall hinged at the toe can be pushed and pulled at the top (causing rotation) by a flexible shaft which is connected to and driven by a variable DC motor and a step-down gear box. The model was made of $\frac{1}{2}$ in. thick aluminum alloy plates (6061-T6) bolted together with gaskets to prevent possible leakage of water during consolidation and loading. One of the side walls was made of 1 in. thick plexiglas for viewing the displacements of the wall-backfill system. The 1 in. thick aluminum rigid retaining wall inside the model box was connected to a brass hinge at the bottom of the wall. Along the vertical center line of the wall six $\frac{1}{2}$ in. diameter

threaded holes were drilled to mount the interface pressure transducers. The dimensions of the box are shown in Figure 1.

B) Sample Preparation: The same kaolin mixture (three parts of Snow-Cal 50 and one part of Mono 90 by weight) was used in preparing the centrifuge model samples and the cylindrical triaxial specimens. The physical properties of the mixture were determined and are tabulated as shown in Table 1. The steps involved in the preparation of a centrifuge model sample are illustrated as follows:

1. A total of 100 pounds of selected air-dry kaolin soil and a fixed amount of distilled water were mixed in the mixer for a period of 12 hours. The mixing was done with extreme care in order not to trap air into the slurry.
2. A layer of sand (Monterey "0") sandwiched between two non-woven geotextile filter sheets was placed at the bottom of the model box for drainage purposes. The well-mixed slurry ($w/c \approx 90\%$) was then poured into the model box behind the retaining wall for consolidation.
3. The initial consolidation of the backfill clay was done on a loading frame with an oil pressure-regulated-loading Piston. Since the fresh slurry cannot carry much load, the first load increment was applied by the self weight of the loading plate. This was followed by staged piston load increments until the consolidation pressure reached 3.0 psi. Each load increment was allowed to last for 12 hours.
4. After completing the initial consolidation, the piston pressure was reduced to zero. Two miniature pore water pressure transducers were then inserted in the model sample at the positions shown in Figure 2. To facilitate this, holes were drilled in the aluminum side wall to

allow a miniature tubular hand auger to bore holes in the sample. After the transducers were properly placed the same kaolin slurry was injected with a long syringe to plug the holes. Water-tight seals were used around the transducer wires and the plugs to insure no leakage of water through the holes. Finally, the pressure on the piston was brought back to the desired consolidation pressure and maintained for a period of 24 hours to re-establish the initial consolidation state of the sample.

5. The model box was then removed from the loading frame and transferred to one of the swing-up platforms in the centrifuge.
6. The flexible cable linking the DC motor was connected to the rigid wall; in addition, an LVDT was mounted near the top of the wall to measure its lateral displacements.
7. Finally, both static and dynamic balancing of the rotating arm were performed to complete the preparation of the model sample for centrifuge testing. Figure 3 shows a complete model placed inside the centrifuge ready to be tested.

C) Instrumentation and Data Acquisition: A microcomputer based data acquisition system (4) was used to monitor the model behavior. The model response was measured by two pore water pressure transducers imbedded in the clay backfill, one LVDT mounted on the rigid wall, and 6 interface pressure transducers installed in and flush with the back side face of the rigid wall. The electric signals were conditioned, picked up in a sequential order by a 16-channel multiplexer, and then fed through a voltage follower which was linked to a pair of slip rings through which the signals are channelled to the outside. A block diagram of the instrumentation and data acquisition scheme is shown in Figure 4. The amount of wall

movement was monitored by the LVDT via the data acquisition system. The movement of the wall was controlled by a variable speed controller that regulates the rpm of the D.C. motor from the outside. In addition, a T.V. monitor permitting continuous viewing of the model during the test was also available.

- D) Model Testing Program and Results: The centrifuge model tests performed for this study involved loading and unloading of the backfill clay soil by pushing and pulling the rigid retaining wall thus causing wall rotation about the hinged bottom. Table 2 presents the sequence of events that took place during a centrifuge model test. As indicated, the model was tested under an equivalent gravitational field approximately 40 times of earth's gravity; during each load increment or decrement segment (field stress initiation, loading and unloading) enough time was allowed for total pore water pressure dissipation. There were four loading segments followed by two unloading segments. In the first segment the initial stress state in the backfill soil was established under the 40-g level. This stress varied from zero at the surface to a maximum at the bottom of the layer; the variation is due to the effect of overburden (and also to a small degree due to the effect of a variable radius of rotation), and can be approximated by a linear variation. During the initial consolidation a uniform effective stress of 3.0 psi was applied throughout the sample as shown in Figure 5a. The effective vertical stress distribution in the clay layer at the 40-g level is represented by the solid line in Figure 5b. The combined 1-g and 40-g consolidation processes cause the clay deposit to develop an overconsolidated zone with varying overconsolidation ratio (OCR) values in the upper portion and a normally consolidation zone below. Since the excess pore water pressure dissipated completely during

the field stress initiation stage, the normal consolidation and over-consolidation zone are clearly defined.

A total of 10 nearly identical model samples were built and tested, however, the earlier tests were invalid, marred by difficulties in data acquisition and/or the leakage of water. Only the last two tests were free from all the possible disorders, thus the results presented herewith are those of "good" tests. A total of approximately 250 minutes was required to carry out a complete centrifuge test; for each test segment (loading or unloading), readings of the pore water pressure and the interface pressure were taken by the automated data acquisition system at specified time intervals.

These data are plotted with time as shown in Figures 6 and 7. Figure 6 depicts the rise and fall of the pore water pressure due to each loading and unloading segment for both transducers. The #1 transducer was embedded at a depth 1.5 in. below the surface of the backfill in the overconsolidated zone; whereas, the #2 transducer was positioned in the normally consolidated zone 4.0 in. below the top of the backfill. Both transducers were placed at a distance of 2 in. behind the rigid wall. The major source of the scatter of measured data is believed to come from the positioning of the transducers as the boreholes may not be perfectly aligned with the positions of the holes on the wall. Figure 7 gives the variations of contact pressure with time under each loading and unloading segment. The pressure registered by the interface pressure transducer was the total pressure including both the pore water pressure and the intergranular soil pressure. Transducer #a was placed very close to the surface of the backfill, thus the readings were very small and not shown in Figure 7.

Based upon the results shown in Figures 6 and 7, a number of observations cited below may be of interest when comparisons are made between the model test results and the finite element analysis prediction.

1. Since the clay is saturated, relatively weak and impervious, an immediate, large excess pore water pressure rise is recorded due to either consolidation or wall movement. This is reflected not only in the pore water pressure readings but also in the total interface pressure readings.
2. With the clay soil as backfill, the resulting total earth pressure behind the wall (after the complete dissipation of excess pore water pressure) does not seem to be affected much by the movement of the wall.
3. There was a separation between the backfill soil and the wall due to unloading (wall moving away from the backfill).

The centrifuge model test results will be compared with the numerical predictions based upon the bounding surface plasticity theory. The following section describes the steps of carrying out the numerical solution for the validation of the plasticity soil model.

MODEL VALIDATION

As stated previously, the model validation was carried out independent of the centrifuge model study. In the entire validation process, the only link relating the model and the numerical solution was the loading, unloading and boundary conditions of the model structure since they serve as input parameters for the analysis. The input parameters for the soil were obtained from laboratory triaxial tests on the same Kaolin clay. The model validation involved the following steps.

1) Laboratory tests for the determination of the bounding surface model parameters. The model parameters were determined from consolidation tests and triaxial tests performed in both compression and extension at three different OCR values. Both manual and computer evaluated calibration procedures have been developed for determining the model parameters from the experimental data as described in references (5,6). For the present study, six isotropically consolidated undrained tests of the Kaolin clay were performed using the automated triaxial testing system developed at Davis (7). Three tests were in extension and three in compression. The results of these tests in terms of q vs ϵ_1 and Δu vs. ϵ_1 , are shown in Figures 8(a,b) and (9a,b) respectively. The results of the consolidation tests are given in Figure 10, which were obtained during the isotropic consolidation process carried out on triaxial specimens prior to undrained shearing.

Since the clay used in this investigation was also used in the previous study of the axisymmetrical problem (storage tank foundation), it is therefore deemed appropriate as a first attempt, to verify the soil behavior according to the bounding surface parameters prescribed for the previous study. Accordingly, the various undrained stress paths in the p' - q space are plotted in Figure 11. The solid lines are predicted stress paths based on the bounding surface soil model, whereas the dots are experimentally determined stress

paths of the current and the previous studies. Note the two sets of lines in extension for OCR 2 and OCR 6 are results from samples consolidated under different pressures. A comparison of the predicted and measured stress paths indicates that they match with each other well, thus, for the current finite element analysis, except for parameters h_c and h_2 , the previously established bounding surface parameters were used. These parameters are tabulated as shown in Table 3. The bounding surface plasticity theory for cohesive soils developed by Dafalias and his co-workers is discussed elsewhere (8,9).

2) The finite element analysis. The description of the 2-D finite element code (SAC-2) can be found in reference (10). As stated previously, the finite element analysis takes into account the actual boundary and loading conditions and the elevated "g-level" experienced in the model, thus, a direct comparison of the model measurements and the theoretical predictions can be made without considering the scaling factors used in the model. The newly developed numerical algorithm for the evaluation of the bounding surface plasticity model for cohesive soils (11) was adopted in the analysis. The robustness of the new algorithm assures accurate results for reasonably sized solution steps and qualitatively corrects predictions, even for exceptionally large steps.

The finite element grid is shown in Figure 12. Since the wall rotates about the hinge, the boundary condition along the rigid retaining wall is complicated. Furthermore when unloading (pulling the wall) takes place a gap may be formed at the interface. When the rotation of the wall is very small it is expected that no slippage takes place and then as the amount of rotation increases slippage between the soil and wall starts from the top and progresses towards the bottom. Finally when pulling of the wall beyond a certain

value the backfill separates from the wall forming a stress (i.e. effective stress) free boundary.

An interface boundary element (based on the theory given in (12)) to account for the soil-structure interaction has been developed and incorporated into the finite element code. It is assumed that the maximum "frictional" stress is determined by the simple Coulomb Law, in which c and f are constants, and even though slippage has taken place, cohesion (when c is specified to be non zero) is maintained. In the present study c and f were taken to be 0.0 and 0.3 respectively.

The interaction of the contacting surfaces is modeled, as shown in Figure 13. In the case when the attainable bond stress has been fully mobilized, the relative movement, δ , is the resulting slippage or separation. When the bond has not broken down, relative movement is resisted by fictitious uniformly distributed bond springs. If the stiffness, k , of the fictitious springs is made large, the relative movement can be made effectively zero. When the maximum attainable tangential bond stress, τ_{\max} , has been developed, slippage is resisted by τ_{\max} applied as loads to the contacting surface. When the soil is contacted with the wall there is no water flow normal to the boundary. However, when separation occurs then a path for water flow exists; this latter effect has been neglected in the present analysis.

A total of 96 time steps were used to perform the computations. The length of the time steps and the number of iterations needed for each step are shown in Table 4. The CPU time on the VAX 750 for running this analysis was about 4 minutes.

COMPARISON OF EXPERIMENTAL AND ANALYTICAL RESULTS

Referring to Figures 6 and 7, the behavior of a model sample during the centrifuge test can be summarized as follows: In the initial consolidation stage, both the pore water pressure and the total lateral pressure built up rapidly in the first 30 seconds of spinning. The magnitude of the measured values were dependent upon the depth of overburden. It took approximately one hour to dissipate the excess pore water pressure and to obtain the full increase in effective stress in the sample; the total pressures measured by the interface pressure cells had the same decreasing trend as did the pore water pressure. During the pushing of the retaining wall both the pore water and the interface pressures were increased and it required about 40 minutes to re-establish the equilibrium state of the system. It was also found that the changes in pressures during pushing and pulling were not greatly affected by the amount of movement of the retaining wall. For instance, the second push increment as shown in Figure 14 was twice that of the first one, however, the pressure increments were not doubled. This phenomenon, is due to the plastic property of the soil. The solid lines in Figures 6 and 7 are results from the finite element analysis, in general they are in good agreement with the experimental results.

In centrifuge testing, the rotating radius varies along the depth of the soil sample, for the present study an average centrifuge gravity, 43g, was adopted and used in the finite element analysis. There is a 7.5% difference in gravity from the general operational table value of 40-g to the adopted average value of 43-g. This correction in gravity considerably improved the predictions of the finite element analysis. While the actual variable gravity over the depth of the sample could be used; it was felt that other uncertainties in the problem did not justify it.

For the bottom interface pressure transducer there is a 15% difference between the prediction and the test results at the end of the first 30 seconds of spinning. This transducer was installed near the bottom of the retaining wall which has a curved end as shown in Figure 2. A finer grid (than the one shown in Figure 12) was used in this area in the finite element analysis to see if any effect of stress concentration could be detected; unfortunately the reasons for this difference are still unknown since the finer grid did not improve the accuracy of the prediction.

CONCLUSION

This report documents the conduct of a complete centrifuge test program of a retaining wall system for the purpose of plasticity theory validation. The triaxial test results were described; the determination and calibration of the bounding surface model parameters were presented.

The experimental phase of the research involved a centrifuge model study of the lateral displacement of a retaining wall having a soft, compressible and saturated clay backfill. The clay deposit was formed from a Kaolin slurry in a rectangular box which was subsequently moved to the centrifuge for further consolidation and "field stress" initiation.

The lateral earth pressures acting on the wall were measured by 6 interface pressure transducers. Two pore water pressure transducers were embedded in the backfill to monitor the rise and dissipation of the pore water pressure resulting from the movement (rotation) of the wall. The wall movement was measured by an LVDT placed on the top of the wall.

The test set-up consisted of a motor driven loading system, and a model package mounted inside the centrifuge. The output signals from the sensors were conditioned and transmitted out of the centrifuge through slip rings. A computer program was written to facilitate the data acquisition scheme.

The second phase of the study involved a comparison of the finite element predictions to the experimentally measured quantities. The program EVAL was used to calibrate the bounding surface model. A friction element was incorporated into SAC-2 to deal with the interface conditions between the retaining wall and the soil mass.

It was found from comparing the results of the tests and the analyses that the total pressures have the same decreasing trend as the pore water pressure during the excess pore water pressure dissipation period, and that the increments during pushing and pulling were not greatly affected by the amount of

movement of the retaining wall. The latter effect clearly demonstrates the importance of plastic deformation.

The study has, as previously stated, broadened the data base for the validation of the bounding surface plasticity model for soft clay. The good agreement obtained between the predictions and the model test results gives further assurance of the versatility and reliability of the constitutive model as well as the finite element analysis method for modeling the behavior of clay soil and its interaction with structures.

REFERENCES

1. Shen, C.K., J. Sohn, K. Mish, V.N. Kaliakin, and L.R. Herrmann, "Centrifuge Consolidation Study for Purposes of Plasticity Theory Validation," ASTM Symposium on Consolidation Behavior of Soils, 1985.
2. Pokrovsky, G.I. and I.S. Fyodorov, "Centrifugal modelling of Construction Works," Isdatelstro Literaturei Pa Stroitelstuu, Moscow, 1968 (translated from the Russian).
3. Cheney, J.A., Lectures notes on Physical Modeling and Introduction to Centrifuge Modeling," Principles of Geotechnical Physical Modeling Workshop, 1982, University of California, Davis.
4. Li, X.S., C.K. Shen, and C.K. Chan, "Microcomputer in Geotechnical Engineering Experiments," Proceedings, 1st National Conference on Microcomputers in Civil Engineering, University of Central Florida, pp. 111-116, Orlando, Florida, October 1983.
5. Dafalias, Y.F., L.R. Herrmann and J.S. DeNatale, "Prediction of the Response of the Natural Clays X and Y Using the Bounding Surface Model," Proceedings of the Workshop on Limit Equilibrium, Plasticity and Generalized Stress-Strain in Geotechnical Engineering, McGill University, ASCE, Part 1, pp. 402-415, May 1980.
6. DeNatale, J.S., L.R. Herrmann, and Y.F. Dafalias, "Calibration of the Bounding Surface Soil Plasticity Model by Multivariate Optimization," Proceedings International Conference on Constitutive Laws for Engineering Materials, University of Arizona, January 1983.
7. Li, X.S., C.K. Chan, and C.K. Shen, "An Automated Triaxial Testing System," ASTM Symposium on Advanced Triaxial Testing of Soil and Rock, June 1986.
8. Dafalias, Y.F. and L.R. Herrmann, "A Bounding Surface Soil Plasticity Model," Proceedings of the International Symposium of Soils Under Cyclic and Transient Loadings, University of Swansea, United Kingdom, pp. 335-345, January 1980.
9. Dafalias, Y.F. and L.R. Herrmann, "Bounding Surface Formulation of Soil Plasticity," Chapter in Soil Mechanics - Transient and Cyclic Loads, John Wiley and Sons, O.C. Zienkiewicz and G.N. Pande, eds., pp. 253-282.
10. Herrmann, L.R. and K.D. Mish, "User's Manual for SAC-2, A Two-Dimensional Nonlinear, Time Dependent Soil Analysis Code Using the Bounding Surface Plasticity Model," Naval Civil Engineering Laboratory, Report CR84.008, December 1983.
11. Herrmann, L.R., V.N. Kaliakin, and C.K. Shen, "Improved Numerical Implementation of the Bounding Surface Plasticity Model for Cohesive Soils," Naval Civil Engineering Laboratory, Report CR86.004 December 1985.
12. Herrmann, L.R., "Finite Element Analysis of Contact Problems," J. Eng. Mech. Div., ASCE, EM5, October 1978.

Table 1
SOIL PROPERTIES

Liquid Limit, LL	37%
Plastic Limit, PL	29%
Shrinkage Limit, SL	26%
* Coefficient of Compressibility, a_v	$(3.96 - 7.92) \times 10^{-3} \text{ m}^2/\text{kN}$
* Coefficient of Permeability, k	$(0.5 - 1.4) \times 10^{-5} \text{ cm/sec}$
* Coefficient of Consolidation, c_v	$3.3 \times 10^{-2} \text{ cm}^2/\text{sec}$

* Determined at consolidation pressures between 27.6 kN/m^2 and 193.2 kN/m^2 .

Table 2. TESTING SEQUENCE

Number	Function	Time (sec)	g-level
1	Start reading	000	1
2	Start spinning	570	1
3	At 40 g	600	40
4	Pushing to .1 in	4200	40
5	End Pushing	4230	40
6	Pushing to .3 in	6600	40
7	End Pushing	6630	40
8	Pushing to .5 in	9000	40
9	End Pushing	9030	40
10	Pulling Back to .3 in	11400	40
11	End Pulling	11430	40
12	Pulling Back to .0 in	13200	40
13	End Pulling	13230	40
14	Stop Spinning	15000	40
15	At 1 g	15030	1
16	End Reading	15600	1

Table 3. PARAMETERS DESCRIBING BOUNDING SURFACE MODEL

Symbol	Description of Property	Value
λ	Slope of isotropic consolidation line for an $e-\ln p'$ plot	0.0745
κ	Slope of elastic rebound line for an $e-\ln p'$ plot	0.0105
M_c	Slope of critical state line in triaxial space (compression)	1.35
R_c	Parameters describing shape of bounding surface (compression)	3.05
A_c		0.175
T		0.010
P_L	Transitional value of confining pressure separating linear rebound curves on $e-\ln p'$ and $e-p'$ plots.	4.4
ν	Poisson's Ratio	0.22
P_a	Atmospheric pressure (used for scaling and establishing units)	101.43 kN/m ²
Γ	Combined bulk modulus for soil particles and pore water	6.9×10^6 kN/m ³
m	Hardening parameter	0.02
h_c	Shape hardening parameter for compression	11
h_2	Shape hardening parameter on the I-axis	9
$n=M_e/M_c$	Ratio of extension to compression values	0.667
$\mu=h_e/h_c$		0.875
$r=R_e/R_c$		0.560
$a=A_e/A_c$		0.850
C	Projection center variable	0.485
S	Elastic zone variable	1.00

Table 4. TIME STEPS IN FINITE ELEMENT ANALYSIS

Function	Time Step (sec)	Iterations
Consolidation		
	100	3
	200	2
	2200	3
Pushing		
	10	3
	87.5	3
	400	2
Pulling		
	3	5
	95	3
	400	2



Figure 3. Model Package in the Centrifuge.

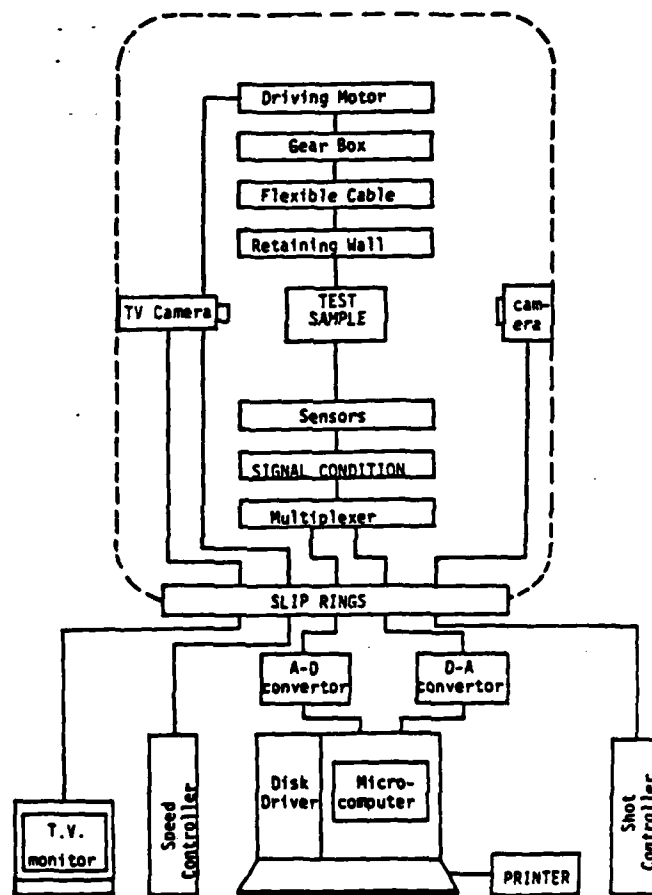


Figure 4. Instrumentation and Data Acquisition Block Diagram.

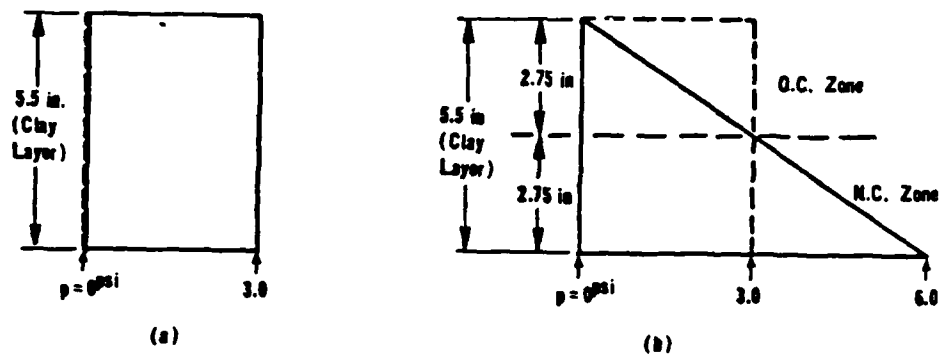


Figure 5. Effective Stress Distributions (a) at 1 g,
(b) at 40 g.

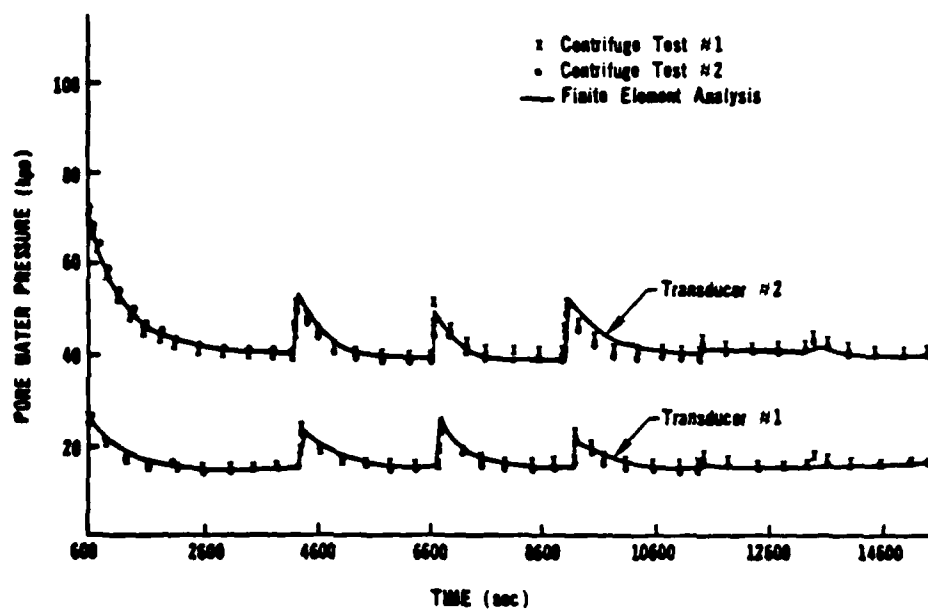


Figure 6. Pore Pressure Response.

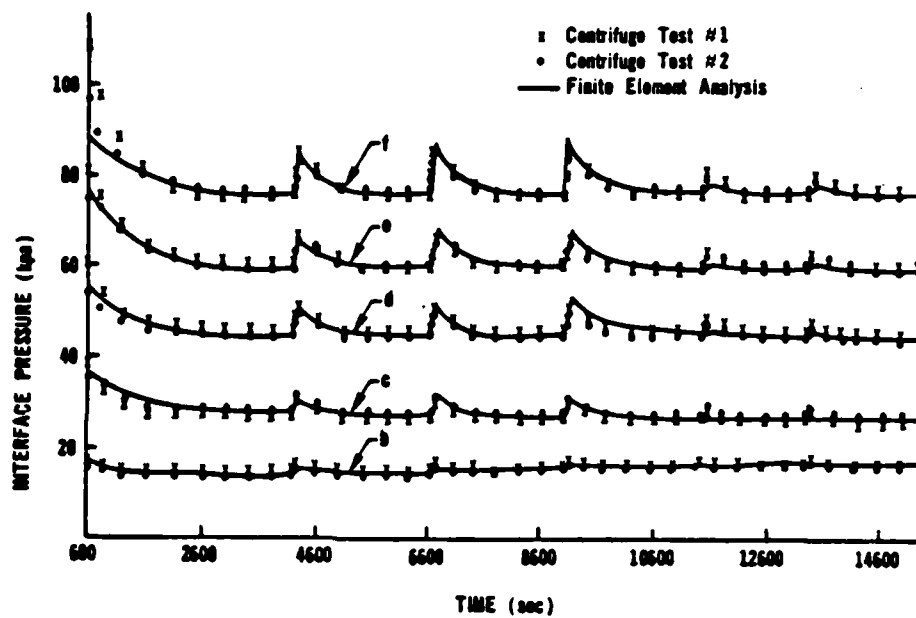


Figure 7. Interface Pressure Response.

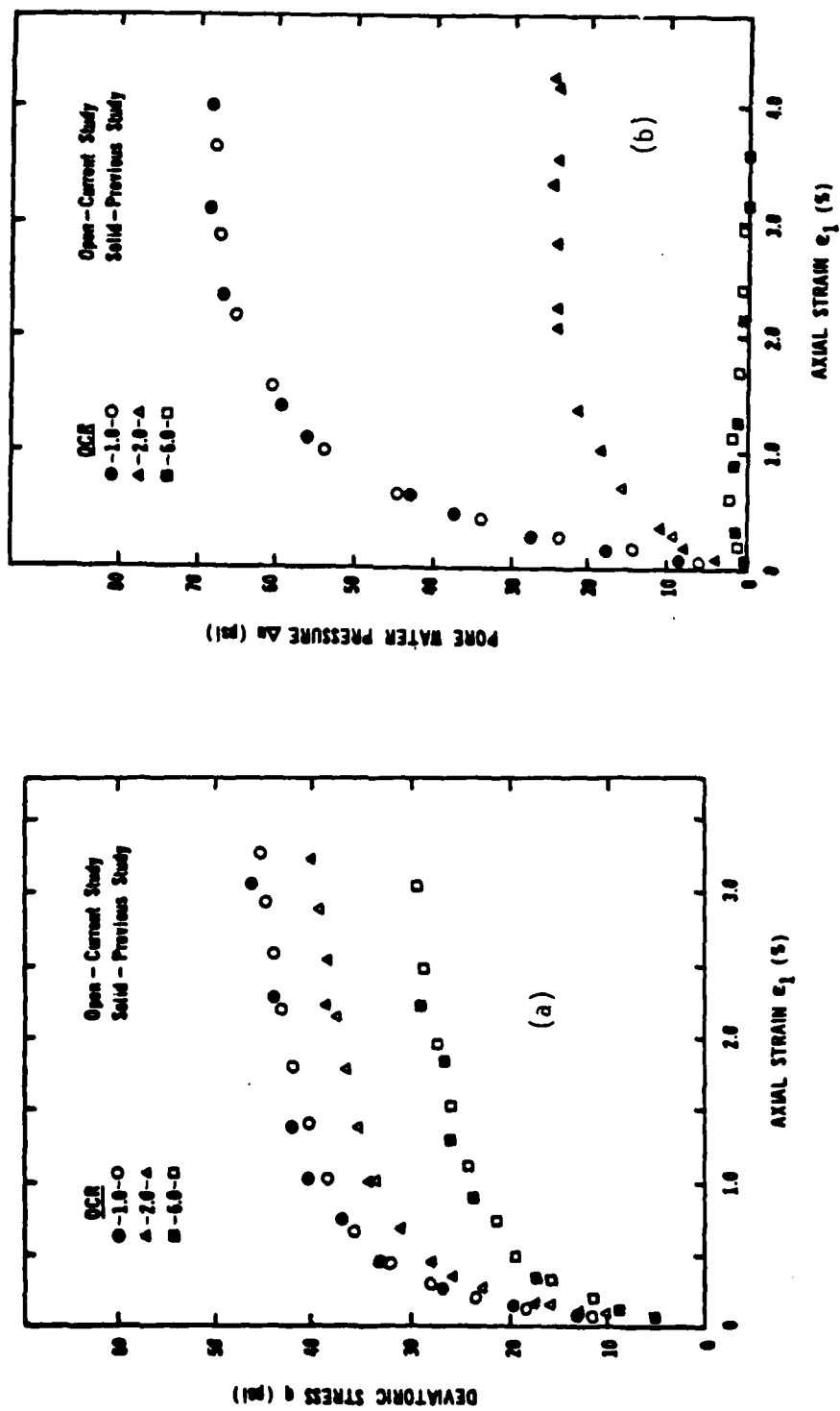


Figure 8. Undrained Compression Test Results
 (a) q vs ϵ_1 , (b) Δu vs ϵ_1

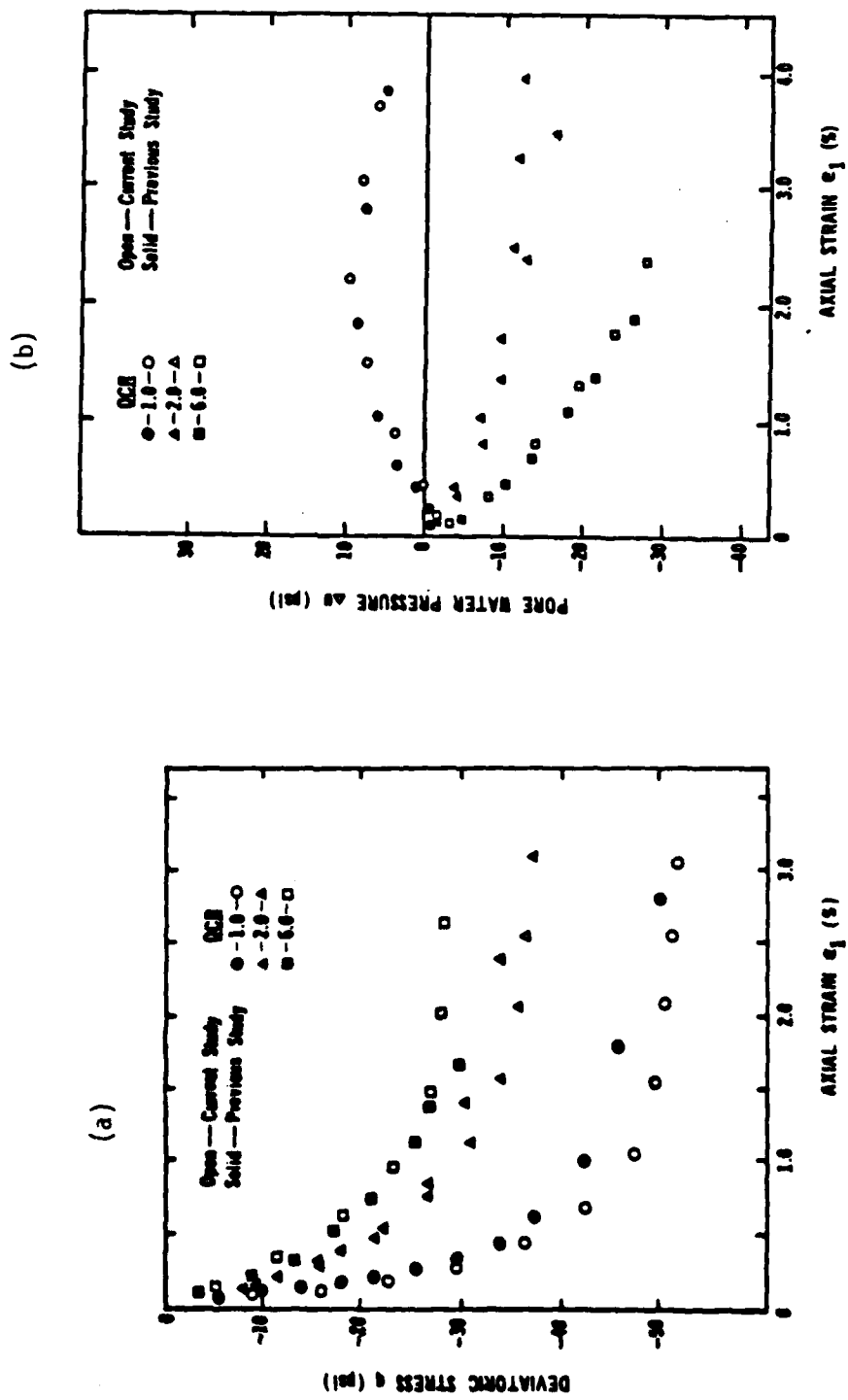


Figure 9. Undrained Extension Test Results
 (a) q vs ϵ_1 , (b) Δu vs ϵ_1

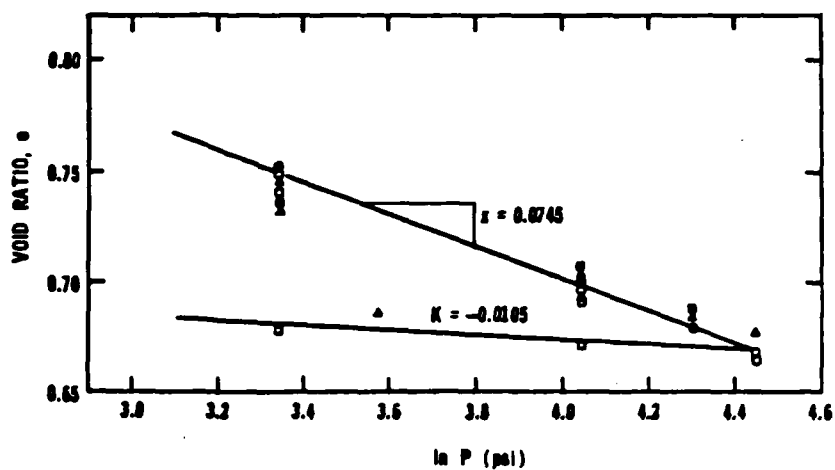


Figure 10. Isotropic Consolidation Results.

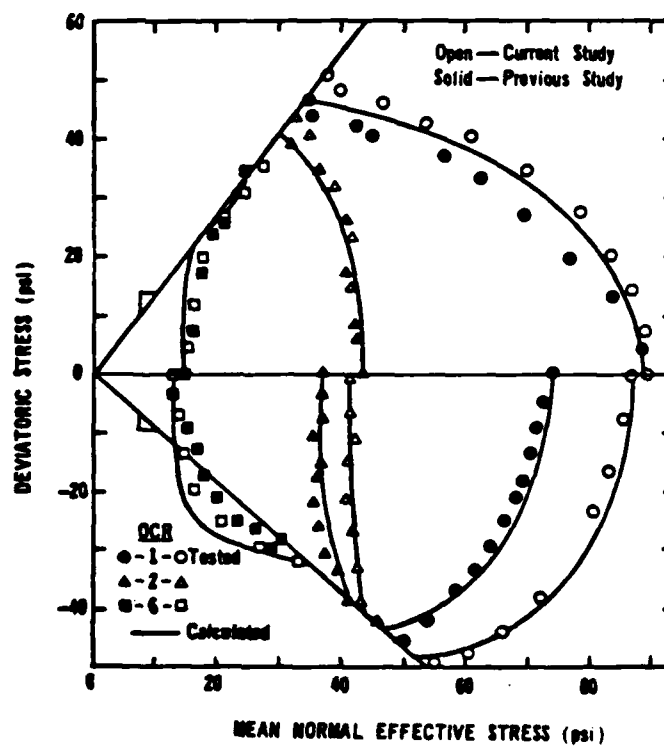


Figure 11. Undrained Stress Paths Under Triaxial Conditions.

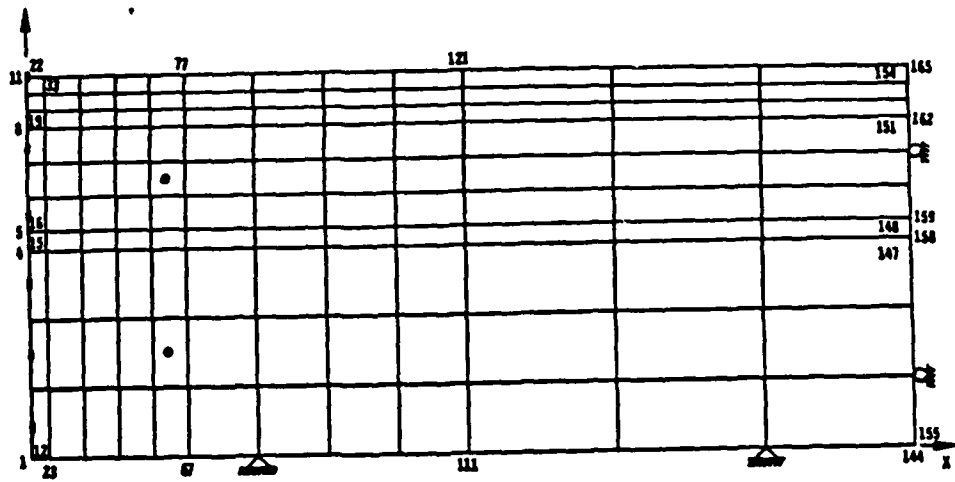


Figure 12. Finite Element Grid.

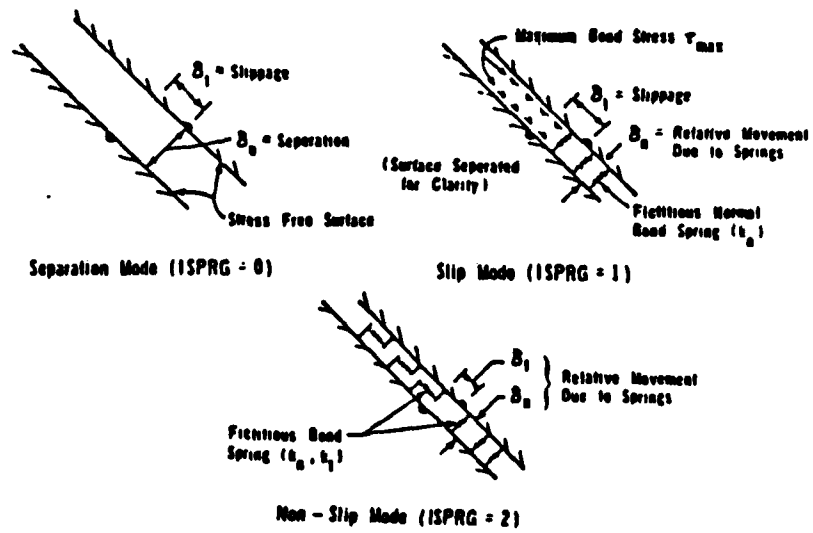


Figure 13. Idealized Model of Bond Between Contacting Surfaces.

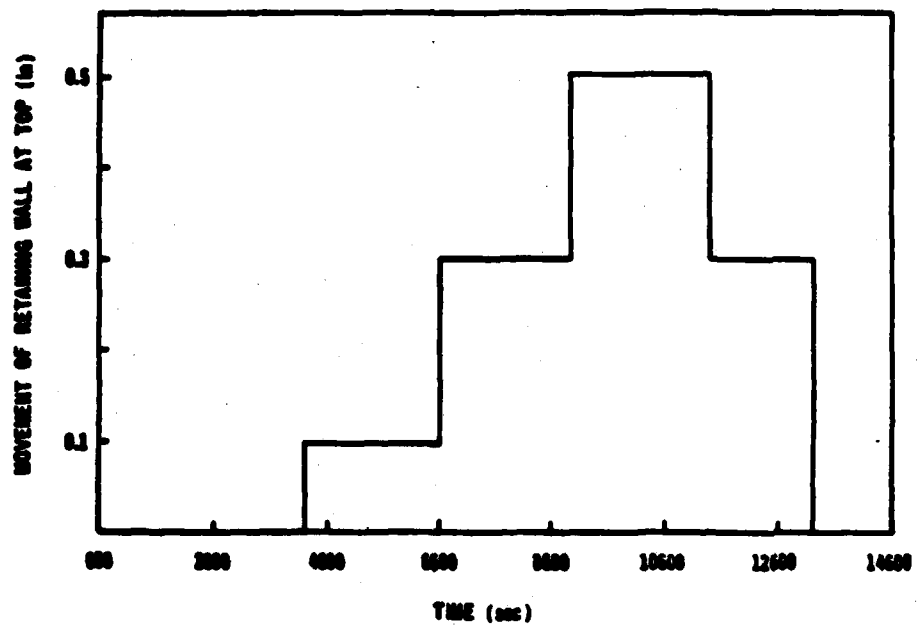


Figure 14. Movement of Retaining Wall.

LIMED
-8